

See discussions, stats, and author profiles for this publication at: <https://www.researchgate.net/publication/225289251>

Cancer Biomarker Detection in Serum Samples Using Surface Plasmon Resonance and Quartz Crystal Microbalance Sensors with Nanoparticle Signal Amplification

ARTICLE in ANALYTICAL CHEMISTRY · JUNE 2012

Impact Factor: 5.64 · DOI: 10.1021/ac300278p · Source: PubMed

CITATIONS

79

READS

196

2 AUTHORS:



Yildiz Uludağ

The Scientific & Technological Research Coun...

19 PUBLICATIONS 352 CITATIONS

SEE PROFILE



Ibtisam E Tothill

Cranfield University

80 PUBLICATIONS 2,403 CITATIONS

SEE PROFILE

Cancer Biomarker Detection in Serum Samples Using Surface Plasmon Resonance and Quartz Crystal Microbalance Sensors with Nanoparticle Signal Amplification

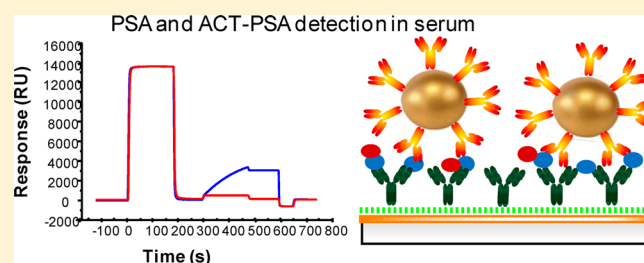
Yildiz Uludag^{†,‡} and Ibtisam E. Tothill^{*,†}

[†]Cranfield Health, Cranfield University, Cranfield, Bedfordshire MK43 0AL, U.K.

[‡]UEKAE–BILGEM, The Scientific and Technological Research Council of Turkey, 41470 Gebze/Kocaeli, Turkey

S Supporting Information

ABSTRACT: Early detection of cancer is vital for the successful treatment of the disease. Hence, a rapid and sensitive diagnosis is essential before the cancer is spread out to the other body organs. Here we describe the development of a point-of-care immunosensor for the detection of the cancer biomarker (total prostate-specific antigen, tPSA) using surface plasmon resonance (SPR) and quartz crystal microbalance (QCM) sensor platforms in human serum samples. K_D of the antibody used toward PSA was calculated as 9.46×10^{-10} M, indicating high affinity of the antibody used in developing the assay. By performing a sandwich assay using antibody-modified nanoparticles concentrations of 2.3 ng mL^{-1} (Au, 20 nm) and 0.29 ng mL^{-1} (8.5 pM) (Au, 40 nm) tPSA in 75% human serum were detected using the developed assay on an SPR sensor chip. The SPR sensor results were found to be comparable to that achieved using a QCM sensor platform, indicating that both systems can be applied for disease biomarkers screening. The clinical applicability of the developed immunoassay can therefore be successfully applied to patient's serum samples. This demonstrates the high potential of the developed sensor devices as platforms for clinical prostate cancer diagnosis and prognosis.



The increase in prostate-specific antigen (PSA) levels in serum above the normal limits (4 ng mL^{-1}) is one of the indications of possible prostate malignancy; therefore, PSA is used as a biomarker for the diagnosis and prognosis of prostate cancer.^{1,2} Prostate-specific antigen is a 34 kDa glycoprotein produced by the prostate gland and is a serine protease enzyme.^{3,4} In serum, PSA is found either in free form or as a complex with protease inhibitor α 1-antichymotrypsin (ACT-PSA, MW 96 kDa), and tPSA refers to the sum of all detectable free and complexed PSA forms.

In the study, the detection of PSA using a label-free optical biosensor was considered that may provide an alternative quick test with respect to the conventional enzyme-linked immunosorbent assay (ELISA)-type testing. One of the most common label-free optical techniques used for biomolecular interaction detection is the surface plasmon resonance (SPR) that takes place when total internal reflection of light occurs at a metal film–liquid interface.^{5,6} SPR causes light energy to be lost to the metal film, and thus, reflected light intensity decreases at a certain resonance angle. This resonance angle is dependent on the local refractive index of the sensor surface.⁷ SPR biosensors have been applied for the detection of PSA in previous studies, and the detection limit of PSA using these systems varies between 0.027 and 1 ng mL^{-1} when PSA is detected in buffer samples.^{8–12} However, to obtain clinically relevant results, it is essential to perform the test in human serum samples.¹³ The main difficulty of using serum as the assay media is the high

nonspecific interaction between the sensor surface and serum proteins. A number of strategies have been adopted in the literature to reduce the nonspecific binding of clinical samples, such as the use of mixed self-assembled monolayer coatings which contain ethylene glycol units, carboxymethyl dextran surface, the use of additives in the assay buffer, the use of blocking agents after antibody immobilization such as milk or certain polymers, and diluting the serum until effects of nonspecific binding are minimized.^{14–16} The methods described above have been applied individually or in combination to reduce the nonspecific binding of serum proteins, hence achieving variable degrees of success. In our study we have used a new matrix elimination buffer which we have developed that eliminates 98% of serum protein nonspecific binding and enables assays in high concentrations of human serum to be conducted.¹⁷

Although optical sensors are highly affected by the optical properties of the detection media, quartz crystal microbalance (QCM) biosensors are not.¹⁸ However, as seen from eq 1 described by Kanazawa, frequency change of QCM sensors is affected by density (ρ_l) and viscosity (η_l) of the detection

Received: January 27, 2012

Accepted: June 3, 2012

Published: June 4, 2012

media (ρ_q = quartz density, f_q = shear modulus, Δf = frequency change):¹⁹

$$\Delta f = -f_q^{3/2} \sqrt{\frac{\rho_l \eta_l}{\pi \rho_q \mu_q}} \quad (1)$$

Although SPR and QCM biosensors allow label-free, direct detection of analytes in buffer, for detection of low concentrations of analytes in clinical samples, performing a sandwich assay is preferable to eliminate the matrix effect of clinical samples such as high refractive index or high viscosity. For example, the injection of serum onto an SPR or QCM sensor chip causes a bulk shift response due to the refractive index (for SPR) and viscosity (for QCM) difference between the running buffer and the serum. If undiluted (or less diluted) serum was used, this high bulk shift response would mask the binding event between the recognition element on the sensor surface and the analyte in serum; hence, no direct assay is possible. However, after washing the serum from the sensor surfaces, the addition of a secondary recognition element such as a detection antibody prepared in buffer will bind to the surface-bound antigen and will provide a measurable signal. Hence, by using a sandwich assay, QCM or SPR assays can be performed in high serum concentrations.

In this study, PSA and ACT–PSA complex in 75% human serum samples were analyzed and compared using both the SPR and QCM biosensors. To be able to detect tPSA at clinically relevant concentrations in serum, detection antibody-modified Au nanoparticles were employed to enhance and amplify the sensor signal. The enhancement of the SPR signals is achieved by increasing the refractive index of the surface further by means of antibody-modified nanoparticles, whereas for the QCM, signal enhancement is achieved as a result of the mass increase due to the use of Au nanoparticles. The use of gold nanoparticles is considered to be better than nanoparticles for SPR signal enhancement because they are biocompatible and denser than other polymeric particles, so they cause higher refractive index changes. Additionally, their ability to cause high resonance angle shift due to their participation in surface plasmon resonance increases the signal further for SPR biosensors.^{20–22} The study results show for the first time that, by the utilization of both matrix buffer and Au nanoparticles, it is possible to detect tPSA in very high serum concentration and at high sensitivity using an SPR biosensor and that the achieved results are comparable to those of the QCM biosensor platform.

■ EXPERIMENTAL SECTION

Materials and Equipment. PSA antibodies were obtained from AbD Serotec, (Kidlington, U.K.). ACT–PSA complex was purchased from BiosPacific (California). Mouse IgG was obtained from Stratech Scientific Ltd. (Newmarket, U.K.). Phosphate-buffered saline (PBS, 0.01 M phosphate buffer, 0.0027 M potassium chloride, and 0.137 M sodium chloride, pH 7.4), bovine serum albumin (BSA), *N*-hydroxysuccinimide (NHS), ethanolamine, and human serum were purchased from Sigma-Aldrich (Poole, U.K.). 1-Ethyl-3-(3 dimethylaminopropyl)-carbodiimide (EDC) was purchased from Pierce-Thermo Scientific (Cramlington, U.K.). The 20 nm Au nanoparticles were purchased from BBIInternational (Cardiff, U.K.), and 40 nm Au nanoparticles were obtained from Diagnostic Consulting Network (California).

A Biacore 3000 (GE Healthcare, Uppsala, Sweden) SPR sensor and QCMA-1 (Sierra Sensors GmbH, Hamburg, Germany) QCM instrument and sensor chips were used for the assays. The operating temperature of the assays was 25 °C, and the flow rate of the buffer was 10 $\mu\text{L min}^{-1}$ for SPR and 80 $\mu\text{L min}^{-1}$ for QCM assays.

Sensor Surface Preparation. Initially bare gold Biacore sensor chips were coated with a self-assembled monolayer by submerging clean gold sensor chips in ethanolic solution of 2 mM mercaptoundecanoic acid overnight. The sensor surfaces were then prepared by immobilizing mouse PSA capture antibody and mouse IgG using conventional amine coupling chemistry.²³ The running buffer used for the immobilization was PBS. Sensor surfaces were first activated with a 1:1 mixture of 400 mM EDC and 100 mM NHS by injecting simultaneously across the sensing spots for 3 min. A 30 $\mu\text{g mL}^{-1}$ PSA capture antibody (in sodium acetate buffer, pH 5.5) was injected on the active channels, and then 30 $\mu\text{g mL}^{-1}$ mouse IgG (in sodium acetate buffer, pH 5.5) was injected on the control channels for 3 min. The surfaces were then blocked with 50 $\mu\text{g mL}^{-1}$ BSA in PBS for 3 min. Nonreacted NHS esters were capped with 1 M ethanolamine, pH 8.5 for 3 min. The response changes were recorded 2 min after the protein injection was completed. The running buffer was changed to PBS buffer containing 0.005% Tween (PBS/T) for the further binding assays.

Modification of Au Nanoparticles with Anti-PSA Detection Antibody. PSA detection antibody was added to the 20 or 40 nm Au nanoparticles solution and incubated at room temperature on a shaker. BSA was added to the solution to ensure that the Au nanoparticles are all coated with antibody or protein. After spinning for 20 min at 4 °C, the antibody-modified nanoparticles were recovered and resuspended in PBS/T buffer. The concentration of nanoparticles was determined by a spectrophotometer at 520 nm wavelength. The antibody-modified Au nanoparticles were then stored in the refrigerator (4 °C) until use.

PSA Detection Assay. In serum, PSA is found either in free form or as a complex with ACT (ACT–PSA, MW 96 kDa). Total PSA (tPSA) refers to the PSA in both forms (PSA and ACT–PSA complex). In the current study to prepare tPSA a 1:1 mixture of PSA and ACT–PSA was used. PSA or tPSA was diluted at specified concentrations (0.29–5000 ng mL^{-1}) in PBS/T buffer containing 5 $\mu\text{g mL}^{-1}$ BSA or 75% human serum (diluted with PBS buffer containing 200 $\mu\text{g mL}^{-1}$ BSA, 0.5 M NaCl, 500 $\mu\text{g mL}^{-1}$ dextran, and 0.5% Tween 20). These solutions were then injected over the PSA capture antibody and mouse IgG immobilized surfaces for 3 min to allow binding interactions. The response changes were recorded 180 s after the PSA/tPSA binding injection was completed. After the binding of PSA/tPSA, the sensor surface was regenerated by injection of 100 mM HCl (1 min, 80 μL) or the assay was continued to perform a sandwich assay.

For the sandwich assay, after the binding of PSA/tPSA to the sensor surface, 1.5 $\mu\text{g mL}^{-1}$ PSA detection antibody or PSA detection antibody-modified Au nanoparticles (20 nm, 5.1×10^{10} nanoparticles/mL or 40 nm, 5.1×10^{10} nanoparticles/mL) was injected on the sensor surface for 3 min (Figure 1). After a 3 min dissociation period under running buffer flow, the surface was regenerated by injection of 100 mM HCl (1 min) and 20 mM NaOH (0.5 min). The frequency changes due to PSA detection antibody binding were recorded 3 min after the injection started.

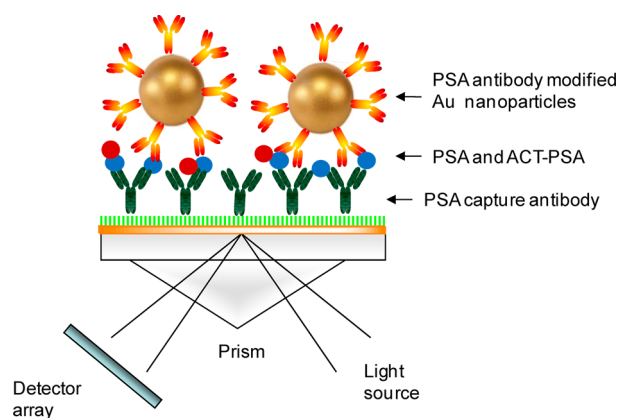


Figure 1. Schematic representation of the PSA sandwich assay using PSA detection antibody-modified Au nanoparticles.

The limit of detection (LOD) was calculated as the signal obtained from the PSA concentration that is equivalent to 3 times the standard deviation of the signals obtained from the blank standards (solutions containing everything except the analyte).

RESULTS AND DISCUSSION

Determination of Nonspecific Binding to the Sensor Surface. Most of the biosensors methods developed for biomarker detection are conducted using spiked buffer samples or 10% serum diluted samples.¹³ In order to develop a clinically relevant procedure, it is essential to validate the assay in human serum. To be able to do this we have developed a new matrix buffer (PBS buffer containing 200 $\mu\text{g mL}^{-1}$ BSA, 0.5 M NaCl, 500 $\mu\text{g mL}^{-1}$ dextran, and 0.5% Tween 20) that enables the elimination of 98% of serum protein nonspecific binding to the sensor surface and allows assays to be carried out in high serum concentration.¹⁷

Initially, the specificity of the detection method was tested by performing several assays using both PSA capture antibody and mouse IgG immobilized SPR sensor surfaces, and the summary of the results is displayed in Table 1. Human serum (75%) was injected on mouse IgG immobilized sensor surface, and subsequent injections of either PSA detection antibody or PSA detection antibody-modified Au nanoparticles showed the degree of nonspecific binding. The nonspecific binding responses were subtracted from the data to get net antigen

binding results, and these are presented in the following sections.

Additionally, 75% human serum was injected over the PSA capture antibody immobilized surface, and subsequent injection of PSA detection antibody (or its Au nanoparticle conjugates) showed the degree of response due to the existing PSA antigen in the commercial serum sample. The concentration of natural PSA in the serum was lower than the detection limit calculated for the sandwich assay. Therefore, there was no difference in the PSA detection antibody binding when it was injected directly to the PSA capture antibody immobilized sensor surface (14 ± 3 RU) or after the serum injection (13 ± 6 RU). However, the detection limit of the sandwich assay with PSA detection antibody-modified Au nanoparticles (20 or 40 nm size) was low; therefore, the binding of the PSA detection antibody-modified Au nanoparticles gave higher responses when it was injected on the sensor surface containing immobilized PSA capture antibodies and serum-injected surfaces with respect to mouse IgG immobilized and serum-injected surfaces. For example, the binding of tPSA detection antibody-modified 40 nm Au nanoparticles after the injection of 75% human serum resulted in 376 ± 10 RU response on PSA capture antibody immobilized surface. A very small part of this signal was nonspecific binding (2 ± 6 RU), whereas the remainder of the signal was due to the tPSA content of the serum obtained from Sigma. When creating the calibration curve, this response was deducted from the responses obtained to get the binding results of the tPSA-spiked serum.

Antibody-Modified Au Nanoparticles. In previous studies it has been shown that antibodies can be simply adsorbed on the Au nanoparticle surface at their isoelectrical point via electrostatic interactions.^{24,25} In the current study, the same procedure was implemented for the modification of the Au nanoparticles with the detection antibody. Although the precise antibody sizes differ, they have been estimated to be in the range of 15–20 nm long and 6–15 nm wide.²⁶ Using these dimensions the footprint of an antibody can be calculated as $2.36 \times 10^{-16} \text{ m}^2$ (length estimated 20 nm, width estimated 15 nm). The approximate number of antibodies on a nanoparticle can be calculated with an assumed packing density of 0.907 (the circle packing density limit)²⁷ using eq 2.

$$\text{no. of antibodies} = 0.907 \frac{\text{nanoparticle surface area}}{\text{antibody footprint area}} \quad (2)$$

The approximate number of antibodies that can fit on a 20 nm nanoparticle was calculated as 5 and on a 40 nm nanoparticle

Table 1. Nonspecific Binding Determination for All Different Assay Formats^a

injected sample	sensor surface			
	mouse IgG immobilized control surface (RU)	PSA capture antibody immobilized active surface (RU)	mouse IgG immobilized and 75% human serum injected control surface (RU)	PSA capture antibody immobilized and 75% human serum injected surface (RU)
5 $\mu\text{g mL}^{-1}$ BSA	8 ± 1	8 ± 6	n/a	n/a
3 $\mu\text{g mL}^{-1}$ anti-PSA detection antibody	4 ± 2	14 ± 3	3 ± 4	13 ± 6
PSA detection antibody-modified 20 nm Au nanoparticles	13 ± 8	52 ± 8	34 ± 6	53 ± 7
PSA detection antibody-modified 40 nm Au nanoparticles			2 ± 6	376 ± 10^b

^aRU: response units; three data points were used to obtain the mean and standard deviation of the results. ^bA very small part of this result was nonspecific binding (2 ± 6 RU), whereas the rest was due to the tPSA content of the serum obtained from Sigma.

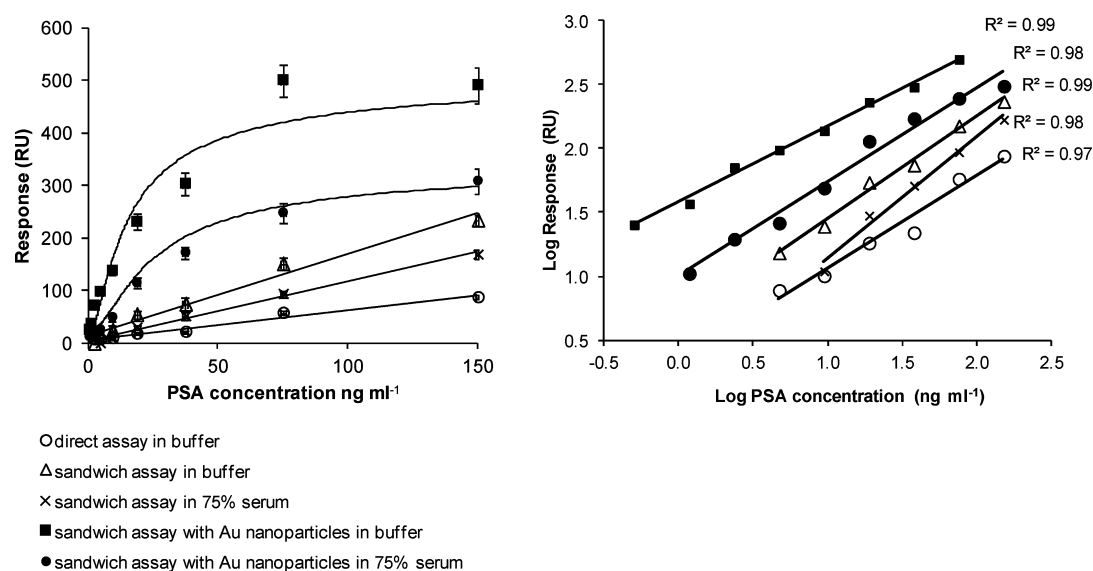


Figure 2. tPSA at varying concentrations (in buffer or in 75% human serum) was injected to tPSA capture antibody immobilized sensor surface. Later, as a sandwich assay tPSA detection antibody or antibody-modified Au nanoparticles were injected, and the responses were recorded and calibration curves (left, linear scale; right, log scale) were obtained.

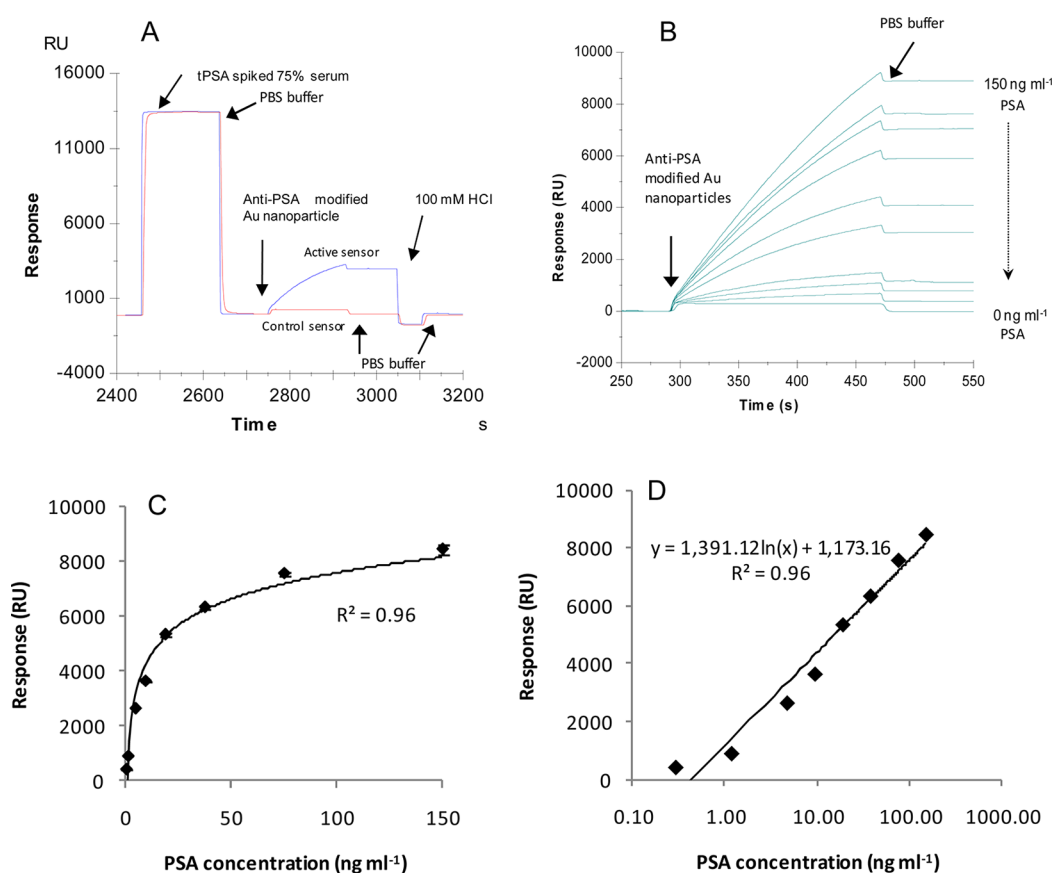


Figure 3. Binding of tPSA antibody-modified Au nanoparticles after the injection of PSA spiked in 75% serum at 9.4 ng mL^{-1} (A) and at varying concentrations from top to bottom in the order of 150, 75, 37.5, 18.8, 9.4 ng mL^{-1} (A), 4.69, 1.17, 0.29, 0 ng mL^{-1} on tPSA antibody immobilized surface and 150 ng mL^{-1} on MIgG-immobilized surface (B). Calibration curves obtained from the assay (C, linear scale; D, log scale).

calculated as 19 using eq 2. Both 20 and 40 nm Au nanoparticles were modified with the PSA detection antibody, and scanning electron microscopy (SEM) images were taken before and after the antibody modification procedure. For the 20 nm Au nanoparticles, the sizes of the nanoparticles were

measured as 16–20 nm before modification, and after antibody modification the sizes were measured between 22 and 31 nm (Supplementary Figure 1 in the Supporting Information). The size differences between the modified and nonmodified nanoparticles were between 6 and 15 nm, not more than the

width of one antibody. Therefore, although theoretically five antibodies can fit on a 20 nm nanoparticle, SEM images indicated that one antibody may be adsorbed on one nanoparticle (20 nm). For the 40 nm Au nanoparticles, SEM image revealed that the sizes of the nanoparticles varied between 20 and 42 nm, and this prevented the comparison of uncoated and antibody-modified nanoparticles. The uncoated Au nanoparticles do coagulate in salt solutions; therefore, the existence of antibody coating on the nanoparticles was confirmed by the addition of salt solution to the Au nanoparticle suspension. The salt-added antibody-modified Au nanoparticle suspension did not coagulate or change color, proving the successful antibody adsorption.

Detection of PSA in 75% Human Serum. One main disadvantage of label-free biosensors such as SPR is the sensitivity of the sensor to any refractive index change of the solutions injected on the sensor surface. Therefore, when testing clinical samples, refractive index mismatch of the buffer, the sample, and the running buffer can become a problem. Although it is possible to use a control serum solution that does not contain elevated levels of the antigen as running buffer, this is not feasible due to cost and health and safety issues. Therefore, performing a sandwich assay instead of a direct assay will help in eliminating this problem. Hence, a sandwich assay approach was followed employing PSA detection antibody-modified Au nanoparticles (20 nm). The buffer containing 200 $\mu\text{g mL}^{-1}$ BSA, 0.5 M salt, 500 $\mu\text{g mL}^{-1}$ dextran, and 0.5% Tween 20 was used to dilute the human serum samples in order to reduce nonspecific binding of human sera proteins on the sensor surface.¹⁷ When tPSA-spiked 75% human serum was injected, a high bulk shift was observed around 12 000 RU due to the high refractive index of the solution (Supplementary Figure 2 in the Supporting Information). This prevents any direct tPSA binding measurements; however, subsequent injection of PSA detection antibody can be detected accurately.

The detection limit of the tPSA assay was improved to 0.5 ng mL^{-1} for the assay in buffer and 2.3 ng mL^{-1} for the assay spiked in 75% human serum by using Au nanoparticles (20 nm) modified with the PSA detection antibody (Figure 2 and Supplementary Table 1 in the Supporting Information).

In most hospitals, the threshold PSA concentration is set as 4 ng mL^{-1} , but recently there has been a tendency to reduce this threshold to 2.5 ng mL^{-1} (mainly in the United States).²⁸ Patients are sent for biopsy if their total PSA level in human serum is above the threshold value. The detection limit of the PSA assay using 20 nm Au nanoparticles is low enough to detect 3.1 ng mL^{-1} in 100% human serum (equivalent of 2.3 ng mL^{-1} in 75% human serum); therefore, the possibility of reducing the LOD further using larger nanoparticles was considered, and for that purpose we repeated the assay using 40 nm Au nanoparticles.

Incorporation of 40 nm Au nanoparticles instead of 20 nm ones lowered the detection limit further to 0.29 ng mL^{-1} (8.5 pM) in 75% human serum (corresponds to 0.39 ng mL^{-1} in 100% serum) (Figure 3).

Although label-free biosensors have several advantages, such as ability of real-time, continuous measurements and no need of a label for sensing, they do have two main disadvantages, and these include limited sensitivity and the requirement of assay optimization and correct use of controls to differentiate nonspecific binding from specific especially when using complex matrixes. In the current study by means of a matrix elimination buffer we minimized the nonspecific sera protein

binding to the sensor surface and performed relative control experiments to confirm the specificity of the antigen bindings. In order to enhance the sensitivity of the sensor to enable the analysis of clinically relevant samples, the use of Au nanoparticles was essential. Au nanoparticles cause high resonance angle shift due to their participation in surface plasmon resonance and hence increase the signal obtained from the sensor.^{20,22} Therefore, the size of the nanoparticle used can have an important effect on the level of signal enhancement.²¹ Larger nanoparticles not only occupy a larger space on the sensor surface that changes the refractive index, but also as the volume of the Au increases its participation to surface plasmon resonance increases, and hence it is expected to enhance sensitivity of the assay further. In our study, although the use of 20 nm Au nanoparticles reduced the detection limit 8 times, the use of 40 nm Au nanoparticles lowered the detection limit 65 times with respect to the sandwich assay. The signal enhancement between 20 and 40 nm nanoparticles is 8 times that correlates very well with the 8 times difference in their volume. Since the detection limit of the tPSA assay is low enough to detect 0.29 ng mL^{-1} (8.5 pM) in 75% human serum (corresponds to 0.39 ng mL^{-1} in 100% serum), it is possible to apply the SPR sensor platform for the determination of total PSA in patient's serum.

Huang et al.¹⁰ performed PSA assay in 50% human serum, and to reduce the nonspecific binding of serum proteins different percentages of thiols were tested to form a mixed self-assembled monolayer (SAM).¹⁰ The optimal mixed SAM concentration was reported to be 10% 16-mercapto-1-hexadecanoic acid, which gave nonspecific binding of ca. 500 RU for 50% human serum. However, the LOD for PSA in 50% human serum was not reported for their work. The authors¹⁰ also reported the use streptavidin-modified gold nanoparticles to enhance the signal and obtained a 1 ng mL^{-1} detection limit for PSA assay in buffer. In another study Cao et al.²⁹ performed a sandwich assay for the detection of PSA–ACT complex using a Biacore 2000, and the detection limit they obtained for PSA–ACT spiked in 10% human serum was 18.1 ng mL^{-1} . Another study performed by Besselink et al.⁸ consisted of two-step signal enhancement process including sandwich assay with rabbit anti-PSA antibodies and then further binding of goat antirabbit IgG-modified Au nanoparticles (10 nm). A 30 min static assay was performed using an IBIS SPR biosensor (IBIS Technologies, Hengelo, Netherlands) and resulted in a LOD of 0.15 ng mL^{-1} for PSA assay in buffer. With respect to the literature mentioned above, the current assay developed in our work shows a high sensitivity with LOD of 0.29 ng mL^{-1} in 75% human serum (6 min total reaction time) using the SPR instrument (Supplementary Table 2 in the Supporting Information).

Additionally, the developed sensor is rapid and has a wide detection range and minimum sample requirement ($\sim 50 \mu\text{L}$); hence, the assay developed in this work outperforms the commercial ELISA kits available for biomarker detection (Supplementary Table 3 in the Supporting Information). For point-of-care testing this type of device can be used in the doctor's surgeries where multiple measurements can be performed using the same sensor. The instrument is fully automated, and samples can be loaded and left to be analyzed. SPR array-type devices are also being developed for future commercial market.

Comparison of the SPR Sensor against a QCM Assay. The results achieved using the SPR sensor for PSA detection

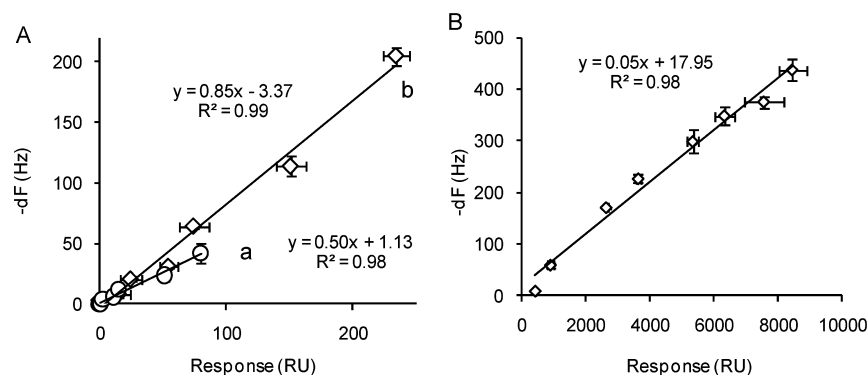


Figure 4. Comparison of the Biacore 3000 (x axis) and QCM-A1 (y axis) results for (A) PSA direct (a) and sandwich assays (b) in buffer and (B) sandwich assay using 40 nm Au nanoparticles in 75% human serum.

were then compared to that achieved previously using a QCM sensor platform.¹⁷ This was carried out in order to confirm and validate the assay conducted on the SPR sensor system. Initially, the interaction kinetic constant for PSA and PSA capture antibody (as a direct assay) was calculated using the data achieved from both the SPR and the QCM biosensors. The simple interaction between an immobilized antibody and an analyte (eq 3) can be described in eq 4, and this equation can be transformed into eq 5, if it is written in terms of biosensor responses [R , sensor response (RU or Hz); C , concentration of analyte (M); k_a , association constant; k_d , dissociation constant].



$$\frac{d[AB]}{dt} = k_a[A][B] - k_d[AB] \quad (4)$$

$$\frac{d[R]}{dt} = k_a C[R_{\max} - R] - k_d R \quad (5)$$

The kinetic data calculations were performed using BIA evaluation software (version 4.1, GE Healthcare) that uses the equations above and enables us to fit the data to interaction models. The PSA binding to the PSA capture antibody immobilized surface was tested in a concentration range between 4.7 and 150 ng mL⁻¹, and PSA binding response curves were then fitted to 1:1 Langmuir binding model to determine the binding association and dissociation rates,³⁰ from which the K_D value was calculated as 9.46×10^{-10} M using the SPR instrument and 5.56×10^{-10} M using the QCM sensor (Supplementary Table 4 in the Supporting Information). The SPR and the QCM results obtained were found to be similar and indicate that the affinity between PSA and PSA capture antibody is in the region of 10^{-10} M. Comparing these results with those achieved by other authors shows that the antibody used had excellent sensitivity. Karlsson et al.³¹ calculated the affinity of anti-PSA antibody toward PSA as 3.3×10^{-9} M (antibody from Fitzgerald Industries Int., clone M212091), whereas Katsamba et al.³² calculated the affinity as 1.1×10^{-9} M (antibody from Fitzgerald Industries Int., clone M612166).

The activity of the QCM and SPR sensor surfaces was evaluated by comparing the theoretical and experimental maximum response obtained from the PSA binding to the immobilized PSA capture antibody. Using the equation listed below (eq 6), the theoretical maximum response can be calculated for the binding of an analyte to a ligand [R_{\max} =

response due to analyte binding; $MW_{\text{analyte/ligand}}$ = molecular weight of analyte (PSA, 33 000 Da) or ligand (PSA antibody, 150 000 Da); R_{ligand} = response obtained from the immobilization of the ligand; V_{ligand} = valency of the ligand, proposed stoichiometry of the interaction].³³

$$R_{\max} = \frac{MW_{\text{analyte}}}{MW_{\text{ligand}}} R_{\text{ligand}} V_{\text{ligand}} \quad (6)$$

After the immobilization of PSA antibody it is expected to have one binding site available to bind to PSA; therefore, V_{ligand} is assumed as 1. For the assay performed using the SPR biosensor, the theoretical R_{\max} calculated as 274 RU using eq 6 and experimental R_{\max} obtained as 110 RU, indicating 40% activity of the antibody-immobilized surface. For the assay performed using the QCM biosensor, the theoretical R_{\max} calculated as 84 Hz using eq 5 and experimental R_{\max} obtained as 108 Hz that corresponds to 129% activity. QCM biosensors are known to be sensitive to the changes in the interfacial chemistry that are associated with biochemical reactions that are instigated at the sensor–liquid interface.³⁴ Hence, it is recorded in the literature that the mass of the analyte calculated using QCM response exceeds the mass response obtained with optical techniques, and this phenomenon is explained due to the viscosity of the buffer between the bound analytes and the rigidity of the analyte layer.³⁵

To compare the assay results of the SPR and the QCM assays further, we plotted the direct and sandwich PSA assay results in buffer using both instruments against each other. Direct and sandwich assay results obtained from the SPR and the QCM instrument produced linear lines with R^2 values of 0.98 and 0.99, respectively (Figure 4A); additionally, sandwich assay in 75% human serum using 40 nm Au nanoparticles gave an R^2 value of 0.98 (Figure 4B). This outcome indicates that the assay results of both instruments are in line with each other and both instruments can be used to detect clinical samples in high serum concentrations.

The results discussed above indicate and confirm that the developed immunoassay enables the detection of PSA in human serum using the SPR sensor and this compares very well with the QCM sensor device developed previously.

CONCLUSION

The PSA test involves the measurement of PSA concentration in serum, and this has been used for the diagnosis and prognosis of prostate cancer patients. In this work, a new immunoassay was developed and applied for an SPR sensor

platform, and this was then compared to a QCM sensor device to detect tPSA in human serum. By using a recently developed matrix elimination buffer, tPSA assay was performed in 75% human serum. With the use of 40 nm Au nanoparticles a detection limit of 0.29 ng mL⁻¹ (8.5 pM) tPSA was obtained in 75% serum which corresponds to 0.39 ng mL⁻¹ in whole serum with the SPR sensor. As this detection limit is lower than the threshold value for prostate cancer detection (2.5 ng mL⁻¹) it is possible to clinically diagnose prostate cancer with the developed immunoassay. Short assay time, repeated usability of the same sensor chip, ability to detect PSA in high serum concentration, and real-time testing enable the application of the optimized assay as a point-of-care device for clinical prostate cancer diagnosis and prognosis.

■ ASSOCIATED CONTENT

■ Supporting Information

Additional information as noted in text. This material is available free of charge via the Internet at <http://pubs.acs.org>.

■ AUTHOR INFORMATION

Corresponding Author

*Phone: + 44(0)7500766487. Fax: + 44(0)1234 758380. E-mail: i.tothill@cranfield.ac.uk.

Notes

The authors declare no competing financial interest.

■ ACKNOWLEDGMENTS

The authors gratefully acknowledge Cranfield Health, Cranfield University, for partial funding of this Ph.D. work.

■ REFERENCES

- (1) Diamandis, E. P. *Trends Endocrinol. Metab.* **1998**, *9*, 310–316.
- (2) Brawer, M. K.; Lange, P. H. *World J. Urol.* **1989**, *7*, 7–11.
- (3) Lilja, H.; Oldbring, J.; Rannevik, G.; Laurell, C. B. *J. Clin. Invest.* **1987**, *80*, 281–285.
- (4) Nash, A. F.; Melezinek, I. *Endocr.-Relat. Cancer* **2000**, *7*, 37–51.
- (5) Rich, R. L.; Myszka, D. G. *Curr. Opin. Biotechnol.* **2000**, *11*, 54–61.
- (6) Pilarik, M.; Vaisocherová, H.; Homola, J. *Methods Mol. Biol. (Clifton, N.J.)* **2009**, *503*, 65–88.
- (7) Fagerstam, L. G.; Frostell-Karlsson, A.; Karlsson, R.; Persson, B.; Ronnberg, I. *J. Chromatogr., A* **1992**, *597*, 397–410.
- (8) Besselink, G. A. J.; Kooyman, R. P. H.; van Os, P. J. H. J.; Engbers, G. H. M.; Schasfoort, R. B. M. *Anal. Biochem.* **2004**, *333*, 165–173.
- (9) Choi, J. W.; Kang, D. Y.; Jang, Y. H.; Kim, H. H.; Min, J.; Oh, B. K. *Colloids Surf., A* **2008**, *313–314*, 655–659.
- (10) Huang, L.; Reekmans, G.; Saerens, D.; Friedt, J.-M.; Frederix, F.; Francis, L.; Muylderms, S.; Campitelli, A.; Hoof, C. V. *Biosens. Bioelectron.* **2005**, *21*, 483–490.
- (11) Schweitzer, B.; Wiltshire, S.; Lambert, J.; O'Malley, S.; Kukanskis, K.; Zhu, Z.; Kingsmore, S. F.; Lizardi, P. M.; Ward, D. C. *Proc. Natl. Acad. Sci. U.S.A.* **2000**, *97*, 10113–10119.
- (12) Yu, F.; Persson, B.; Lofas, S.; Knoll, W. *Anal. Chem.* **2004**, *76*, 6765–6770.
- (13) Homola, J. *Chem. Rev.* **2008**, *108*, 462–493.
- (14) Ayela, C.; Roquet, F.; Valera, L.; Granier, C.; Nicu, L.; Pugnière, M. *Biosens. Bioelectron.* **2007**, *22*, 3113–3119.
- (15) Situ, C.; Wylie, A. R. G.; Douglas, A.; Elliott, C. T. *Talanta* **2008**, *76*, 832–836.
- (16) Trevino, J.; Calle, A.; Rodriguez-Frade, J. M.; Mellado, M.; Lechuga, L. M. *Talanta* **2009**, *78*, 1011–1016.
- (17) Uludag, Y.; Tothill, I. E. *Talanta* **2010**, *82*, 277–282.
- (18) Cooper, M. A.; Singleton, V. T. *J. Mol. Recognit.* **2007**, *20*, 154–184.
- (19) Kanazawa, K. K. *Faraday Discuss.* **1997**, *77*–90.
- (20) Lyon, L. A.; Musick, M. D.; Smith, P. C.; Reiss, B. D.; Pena, D. J.; Natan, M. J. *Sens. Actuators, B* **1999**, *54*, 118–124.
- (21) Mustafa, D. E.; Yang, T. M.; Xuan, Z.; Chen, S. Z.; Tu, H. Y.; Zhang, A. D. *Plasmonics* **2010**, *5*, 221–231.
- (22) Lyon, L. A.; Pena, D. J.; Natan, M. J. *J. Phys. Chem. B* **1999**, *103*, 5826–5831.
- (23) Fischer, M. J. E. In *Surface Plasmon Resonance: Methods and Protocols*; DeMol, N. J., Fischer, M. J. E., Eds.; Humana Press Inc.: Totowa, NJ, 2010; Vol. 627, pp 55–73.
- (24) West, J. L.; Halas, N. J. *Curr. Opin. Biotechnol.* **2000**, *11*, 215–217.
- (25) Zeng, S.; Yong, K.-T.; Roy, I.; Dinh, X.-Q.; Yu, X.; Luan, F. *Plasmonics* **2011**, *6*, 491–506. DOI: 10.1007/s11468-011-9228-1.
- (26) Kreier, J. P. *Infection, Resistance and Immunity*; Taylor & Francis: New York, NY, 2002.
- (27) Schwartz, J. J.; Quake, S. R. *Appl. Phys. Lett.* **2007**, *91*, 083902.
- (28) Hamdan, M. H. *Cancer Biomarkers*; John Wiley & Sons Inc.: Hoboken, NJ, 2007.
- (29) Cao, C.; Kim, J. P.; Kim, B. W.; Chae, H.; Yoon, H. C.; Yang, S. S.; Sim, S. J. *Biosens. Bioelectron.* **2006**, *21*, 2106–2113.
- (30) Rich, R. L.; Myszka, D. G. In *Label-Free Biosensors Techniques and Applications*; Cooper, M., Ed.; Cambridge University Press: New York, NY, 2009.
- (31) Karlsson, R.; Katsamba, P. S.; Nordin, H.; Pol, E.; Myszka, D. G. *Anal. Biochem.* **2006**, *349*, 136–147.
- (32) Katsamba, P. S.; Navratilova, I.; Calderon-Cacia, M.; Fan, L.; Thornton, K.; Zhu, M.; Bos, T. V.; Forte, C.; Friend, D.; Laird-Offringa, I.; Tavares, G.; Whatley, J.; Shi, E.; Widom, A.; Lindquist, K. C.; Klakamp, S.; Drake, A.; Bohmann, D.; Roell, M.; Rose, L.; Dorocke, J.; Roth, B.; Luginbühl, B.; Myszka, D. G. *Anal. Biochem.* **2006**, *352*, 208–221.
- (33) *Sensor Surface Handbook*; GE Healthcare-Biacore: Buckinghamshire, UK, 2003; p 96.
- (34) Sheikh, S.; Blaszykowski, C.; Thompson, M. *Anal. Lett.* **2008**, *41*, 2525–2538.
- (35) Hook, F.; Voros, J.; Rodahl, M.; Kurrat, R.; Boni, P.; Ramsden, J. J.; Textor, M.; Spencer, N. D.; Tengvall, P.; Gold, J.; Kasemo, B. *Colloids Surf., B* **2002**, *24*, 155–170.